Systems & Control Letters 59 (2010) 663–670

Contents lists available at ScienceDirect

Systems & Control Letters

journal homepage: www.elsevier.com/locate/sysconle

Smooth weight optimization in $\mathscr{H}_\infty$ loop-shaping design

M. Osinuga *, S. Patra, A. Lanzon

Control Systems Centre, School of Electrical and Electronic Engineering, University of Manchester, Sackville Street, Manchester M13 9PL, United Kingdom

ARTICLE INFO

Article history:
Received 14 September 2009
Received in revised form
19 July 2010
Accepted 23 July 2010
Available online 21 September 2010

Keywords:
$\mathscr{H}_\infty$ loop-shaping
Smoothness constraint
Weight optimization
Robust control

ABSTRACT

Smooth variation in the magnitude response of weights facilitates $\mathscr{H}_\infty$ loop-shaping design, as it prevents the cancellation of important modes of the system, for example, lightly damped poles/zeros of flexible structures, when the shaped plant is formed based on closed-loop design specifications. For accurate fitting of transfer functions to magnitude data, smooth weights also allow low-order transfer functions to be used when such smooth variations in their magnitude responses are computed point-wise in frequency. In this paper, smoothness constraints for weights, expressed as gradient constraints on a log scale in dB/decade, which is intuitive from a design perspective, are imposed in a weight optimization framework for $\mathscr{H}_\infty$ loop-shaping control. This work builds on [A. Lanzon, Weight optimization in $\mathscr{H}_\infty$ loop-shaping, Automatica 41 (1) (2005) 1201–1208], where additional constraints are formulated in linear matrix inequality (LMI) form to cast a complete weight optimization framework. The resulting algorithm thus maximizes the robust stability margin and simultaneously synthesizes smooth weights along with a stabilizing controller. A numerical example is given to elucidate the efficacy of the smoothness constraints in $\mathscr{H}_\infty$ loop-shaping control.

1. Introduction

$\mathscr{H}_\infty$ loop-shaping control is a design paradigm that establishes a good trade-off between robust stability and robust performance of a closed-loop system by combining classical loop-shaping concepts with $\mathscr{H}_\infty$ synthesis. In Fig. 1, the design framework is depicted where a stabilizing controller C_∞ is synthesized based on the shaped plant $P_s = W_2PW_1$; then the final $\mathscr{H}_\infty$ loop-shaping controller is obtained by cascading weights with the stabilizing controller C_∞ to give the controller $C = W_1C_\infty W_2$, which will be implemented on the plant P. Let $\mathscr{C}(P_s)$ be the set of all stabilizing controllers for P_s, i.e. $\mathscr{C}(P_s) := \{C_\infty : [P_s, C_\infty] \text{ is internally stable}\}$. The robust stability margin $b(P_s, C_\infty)$ is then defined as

$$b(P_s, C_\infty) := \left\| \begin{bmatrix} P_s \\ I \end{bmatrix} (I - C_\infty P_s)^{-1} \begin{bmatrix} -C_\infty & I \end{bmatrix} \right\|_\infty^{-1}$$

if $[P_s, C_\infty]$ is internally stable or as $b(P_s, C_\infty) := 0$ otherwise. (1)

The maximum achievable robust stability margin is defined as $b_{\text{opt}}(P_s) := \sup_{C_\infty} b(P_s, C_\infty)$, where $b_{\text{opt}}(P_s) \leq 1$ for any P_s [1].

A designer's objective is to maximize the robust stability margin $b(P_s, C_\infty)$ by synthesizing a stabilizing controller C_∞ for the shaped plant P_s which is formed beforehand through proper weight selection based on closed-loop requirements. It is worth mentioning that weight selection depends on many factors such as the right-half plane (RHP) poles/zeros of the nominal plant, strength of cross-coupling for multi-input multi-output (MIMO) systems, roll-off rate around cross-over, singular values and condition numbers of the loop-shaping weights, and so on. All of these issues have been discussed in detail in [2–5]. In [5], these factors have been combined into a single optimization framework that facilitates design in that it gives an algorithm for simultaneously synthesizing weights and a stabilizing controller that maximize the optimal robust stability margin.

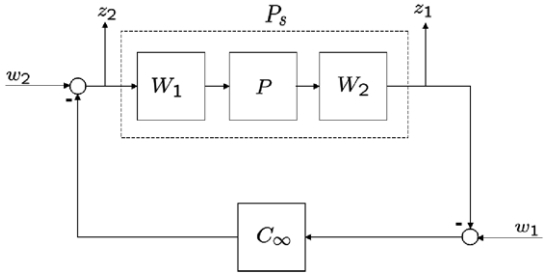

Fig. 1. Feedback interconnection.

This algorithm [5] is computationally efficient as the optimization problem is posed in quasi-convex form to design either diagonal or non-diagonal weights and is easily implementable using available LMI toolbox. Although this algorithm works well for

* Corresponding author. Tel.: +44 161 3062821; fax: +44 161 306 9341.
E-mail addresses: mobolaji.osinuga-2@postgrad.manchester.ac.uk, olefemmy@yahoo.com (M. Osinuga), sourav.patra@manchester.ac.uk (S. Patra), alexander.lanzon@manchester.ac.uk (A. Lanzon).

0167-6911/$ – see front matter © 2010 Elsevier B.V. All rights reserved.
doi:10.1016/j.sysconle.2010.07.011

Notation

$\mathbb{R}, \mathbb{R}_+, \mathbb{R}_+^n$ Respectively the set of real numbers, the set of strictly positive real numbers and the set of column vectors of dimension $(n \times 1)$, each of n entries in $\mathbb{R}_+$.

$\mathscr{R}^{n\times m}$ Set of real rational transfer function matrices of dimension $(n \times m)$.

$\mathscr{RH}_\infty{}^{n\times m}$ Set of real rational stable transfer function matrices of dimension $(n \times m)$.

$\mathscr{GH}_\infty$ Function space that are units in $\mathscr{RH}_\infty$ (i.e. $f \in \mathscr{GH}_\infty \Leftrightarrow f, f^{-1} \in \mathscr{RH}_\infty$).

$\sigma_i(A)$ The i-th singular value of matrix A.

$\overline{\sigma}(A)$ (resp. $\underline{\sigma}(A)$) Largest (resp. smallest) singular value of matrix A.

$\kappa(A)$ Condition number of matrix A, defined as $\kappa(A) := \overline{\sigma}(A)/\underline{\sigma}(A)$.

$\mathrm{diag}\begin{pmatrix} a \\ b \end{pmatrix}$ Shorthand notation for $\begin{pmatrix} a & 0 \\ 0 & b \end{pmatrix}$.

$\mathbf{\Lambda}_n$ Set of real strictly positive diagonal matrices of dimension $(n \times n)$, defined as $\mathbf{\Lambda}_n := \{\mathrm{diag}(x) : x \in \mathbb{R}_+^n\}$.

almost all LTI systems, it does not mitigate against stable[1] lightly damped pole-zero cancellation when the shaped plant is formed for lightly damped systems. This is an important factor in design as it affects the robust performance and robust stability of the closed-loop system [4,6–10].

To illustrate this fact, let us consider an example of a spring–mass system whose transfer function is given as $P(s) = \frac{k}{s^2(M_1M_2s^2+(M_1+M_2)k)}$ [11, Section 6.1]. The system is shown in Fig. 2(a) and is based on measurements of the position of the second mass M_2. It has a rigid-body mode (M_1 and M_2 constrained to a rectilinear motion without friction) and a single vibration mode (spring of stiffness k). Using nominal values of $M_1 = M_2 = 1$ kg and $k = 1$ N m^{-1}, the nominal plant's transfer function is obtained as $P_0(s) = \frac{1}{s^2(s^2+2)}$, where $P_0(s)$ has two undamped poles at $s = \pm j\sqrt{2}$. The algorithm of Lanzon [5] can then be used to shape the singular values of the nominal plant via weight synthesis; the resulting singular value plots of the nominal and shaped plant are shown in Fig. 2(b). From these plots, it is apparent that the synthesized weight cancels the undamped modes of the nominal plant. From a design perspective, this is undesirable as it results in poor robustness of the closed-loop system and is therefore a shortcoming of the algorithm, which we will remove in this paper.

Flexible structures are unique and challenging (see [12,13] and the references therein), and as illustrated above, the algorithm of Lanzon [5], when used to design weights for this class of system, cannot guarantee the avoidance of stable pole-zero cancellations of the lightly damped/undamped modes of the system. In this paper, this drawback has been circumvented by introducing smoothness constraints (on the synthesized weights) into the aforementioned weight optimization framework. This 'smoothness' implies a placid or gentle slope in the magnitude plot of weights which prevents stable pole-zero cancellation in the shaped plant. In the proposed algorithm, the smoothness constraints are imposed as gradient constraints on a log scale in dB/decade, which is relevant from a design perspective. More importantly, the constraints are formulated in LMI form so that they can be directly added to the algorithm of Lanzon [5] to obtain a complete weight optimization framework for $\mathscr{H}_\infty$ loop-shaping control. Hence, this modified algorithm extends its applicability to all LTI systems, including lightly damped and undamped plants. The algorithm proposed in this paper is formulated to synthesize only diagonal weights, which is consistent with the observation that diagonal weights are generally sufficient to shape the singular values of the nominal plant. However, with minor modifications as discussed in [5], it is very easy to extend this work to smooth non-diagonal weights synthesis.

[1] Note that there is no possibility of unstable pole-zero cancellation using the discussed algorithm since stable minimum phase transfer functions are fitted as loop-shaping weights.

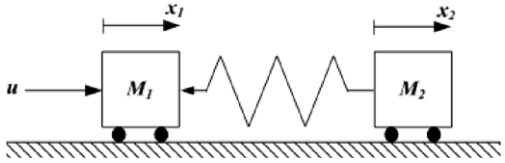

(a) Schematic diagram of a spring–mass system.

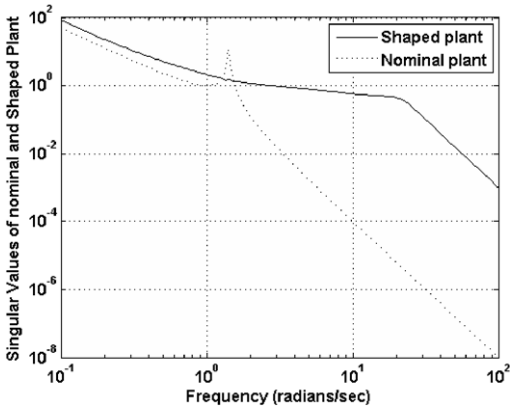

(b) Singular values of P_s and P.

Fig. 2. Spring–mass system and singular value plots of P_s and P.

The rest of the paper is organized as follows. As background of the present work and in order to define the notation and preliminaries, a brief description of the weight optimization problem of Lanzon [5] is given in Section 2, while the proposed smoothness constraints are formulated in Section 3. The solution algorithm is detailed in Section 4 and in Section 5, a numerical example is shown to illustrate the effectiveness of the proposed algorithm. Section 6 concludes the paper.

2. Weight optimization problem of Lanzon [5]

Here, we briefly describe the weight optimization framework of Lanzon [5] in order to define the notation and the underpinning mathematical machinery. For a scaled plant $P \in \mathscr{R}^{m\times n}$, where $m \geq n$,

$$\text{define} \quad \Lambda_{1\omega} = W_1(j\omega)^{-*}W_1(j\omega)^{-1} \in \mathbf{\Lambda}_n \quad \text{and} \quad \Lambda_{2\omega} = W_2(j\omega)^{*}W_2(j\omega) \in \mathbf{\Lambda}_m. \tag{2}$$

The following set is also defined for compactness of notation:

$$\mathbf{\Xi}(\alpha, \beta, \zeta) := \{W \in \mathscr{GH}_\infty : \alpha(\omega) < \sigma_i(W(j\omega)) < \beta(\omega), \kappa(W(j\omega)) < \zeta(\omega)\ \forall i, \omega\}$$

for some given continuous functions $\alpha, \beta, \zeta : \mathbb{R} \to \mathbb{R}_+$ that satisfy $\beta(\omega) > \alpha(\omega)$ and $\zeta(\omega) > 1\ \forall\omega$. The frequency functions α and β delimit the allowable region for the singular values of W, and ζ is a frequency function that provides a bound for the condition number of W.

The optimization problem was posed in [5] as follows:

$$\max_{\substack{W_1\in\Xi(\underline{w}_1,\overline{w}_1,k_1)\\ W_2\in\Xi(\underline{w}_2,\overline{w}_2,k_2)}} b_{\text{opt}}(P_s)$$

$$\text{subject to } \underline{s}(\omega) < \sigma_i(P_s(j\omega)) < \bar{s}(\omega)\ \forall i,\omega, \tag{3}$$

where the frequency functions $\underline{s}(\omega)$ and $\bar{s}(\omega)$ are the boundaries for an allowable loop shape. $\underline{s}$, $\bar{s}$, $\underline{w}_i$, $\overline{w}_i$ and k_i $(i = 1, 2)$ are continuous real-valued positive functions of frequency, specified by the designer.

The above optimization problem seeks to maximize the optimal robust stability margin and therefore does not depend on any particular controller. Using the definition of $b(P_s, C_\infty)$ given in (1) and performing some algebraic manipulations, the optimization problem, dropping the dependence on $j\omega$ for the purpose of brevity, is formulated as follows.

Minimize γ^2

such that $\exists C \in \mathscr{C}(P)$ and $\forall\omega\ \exists\ \Lambda_{1\omega} \in \mathbf{\Lambda}_n$ and $\Lambda_{2\omega} \in \mathbf{\Lambda}_m$ satisfying

$$\text{(a) } \begin{bmatrix}0 & P\\ 0 & I\end{bmatrix}^* \begin{bmatrix}\Lambda_{2\omega} & 0\\ 0 & \Lambda_{1\omega}\end{bmatrix}\begin{bmatrix}0 & P\\ 0 & I\end{bmatrix} \le \gamma^2 \begin{bmatrix}I & P\\ C & I\end{bmatrix}^* \begin{bmatrix}\Lambda_{2\omega} & 0\\ 0 & \Lambda_{1\omega}\end{bmatrix}\begin{bmatrix}I & P\\ C & I\end{bmatrix},$$

$$\text{(b) } \underline{s}(\omega)^2\Lambda_{1\omega} < P^*\Lambda_{2\omega}P < \bar{s}(\omega)^2\Lambda_{1\omega},$$

$$\text{(c) } \exists \underline{\xi}_{1\omega}, \overline{\xi}_{1\omega} : \underline{\xi}_{1\omega} I < \Lambda_{1\omega} < \overline{\xi}_{1\omega} I, \overline{w}_1(\omega)^{-2} < \underline{\xi}_{1\omega},\ \overline{\xi}_{1\omega} < \underline{w}_1(\omega)^{-2},\ \overline{\xi}_{1\omega} < k_1(\omega)^2\underline{\xi}_{1\omega},$$

$$\text{(d) } \exists \underline{\xi}_{2\omega}, \overline{\xi}_{2\omega} : \underline{\xi}_{2\omega} I < \Lambda_{2\omega} < \overline{\xi}_{2\omega} I, \underline{w}_2(\omega)^2 < \underline{\xi}_{2\omega},\ \overline{\xi}_{2\omega} < \overline{w}_2(\omega)^2,\ \overline{\xi}_{2\omega} < k_2(\omega)^2\underline{\xi}_{2\omega}.$$

The above optimization problem is quasi-convex when the controller $C \in \mathscr{C}(P)$ is held fixed. Here, inequality (a) captures the design objective for maximizing $b(P_s, C_\infty)$ while (b) delimits the singular values of the shaped plant P_s within the specified loop-shape boundaries $\underline{s}$ and $\bar{s}$, which are chosen by the designer based on closed-loop specifications. In addition, (c) and (d) provide bounds on the singular values and condition numbers of the synthesized loop-shaping weights. The above optimization problem is posed to synthesize diagonal weights only, which is a specialized form of the formulation in [5], obtained by replacing unitary matrices with the identity matrix.

3. Formulation of the smoothness constraints for weights

The objective of this paper is to ensure smoothness of the synthesized loop-shaping weights by imposing constraints on the gradient of the weights' magnitude responses. The constraints are expressed in LMI form so that they can be fitted into the existing algorithm given in the previous section in order to design smooth weights and a stabilizing controller for $\mathscr{H}_\infty$ loop-shaping control. Now, we will show the mathematical formulation of the smoothness constraints for compensators W_1 and W_2. To formulate the constraints, we consider the magnitude response of the weight and its gradient between two points that are very close to each other. It is intuitive for any practising engineer to express these constraints on a log–log scale (i.e. $20\log_{10}|W_i|$ $(i = 1, 2)$ with respect to $\log_{10}\omega$) as it is consistent with the notation (dB/decade) used in Bode plots for single-input single-output (SISO) systems and singular value plots for MIMO systems.

For a diagonal transfer function matrix $W \in \mathscr{GH}_\infty{}^{p\times p}$, we further define the following set for compactness of notation:

$$\mathbf{\Pi}(\alpha,\beta,\zeta,\eta) := \left\{ W = \text{diag}\begin{pmatrix}w_1\\ w_2\\ \vdots\\ w_p\end{pmatrix} \in \mathscr{GH}_\infty{}^{p\times p} : \right.$$
$$\alpha(\omega) < \sigma_i(W(j\omega)) < \beta(\omega),\ \kappa(W(j\omega)) < \zeta(\omega),$$
$$\left.\left|\frac{\mathrm{d}}{\mathrm{d}(\log_{10}\omega)}(20\log_{10}|w_i(j\omega)|)\right| < \eta(\omega)\ \forall\omega, i = 1, 2, \ldots, p\right\}$$

for some given continuous functions $\alpha,\beta,\zeta,\eta : \mathbb{R} \to \mathbb{R}_+$ that satisfy $\beta(\omega) > \alpha(\omega)$, $\zeta(\omega) > 1$ and $\eta(\omega) > 0\ \forall\omega$. The frequency function η, expressed in dB/decade, provides a bound for the gradient of the magnitude response of w_i $(i = 1, 2, \ldots, p)$. The optimization problem posed in the previous section can now be rewritten to include bounds on the gradient of the magnitude response of the compensators as follows:

$$\max_{\substack{W_1\in\mathbf{\Pi}(\underline{w}_1,\overline{w}_1,k_1,g_1)\\ W_2\in\mathbf{\Pi}(\underline{w}_2,\overline{w}_2,k_2,g_2)}} b_{\text{opt}}(P_s)$$

$$\text{subject to } \underline{s}(\omega) < \sigma_i(P_s(j\omega_j)) < \bar{s}(\omega)\ \forall i,\omega, \tag{4}$$

where $\underline{s}$, $\bar{s}$, $\underline{w}_i$, $\overline{w}_i$, k_i and g_i $(i = 1, 2)$ are continuous real-valued positive frequency functions. We derive a constraint for the first diagonal element of the weight; the constraints for all diagonal elements are thereafter combines to obtain a smoothness constraint for the MIMO weight in LMI form. For simplicity, we denote $\log_{10}\omega$ as ν_ω.

3.1. Smoothness constraint for diagonal pre-compensator $W_1(j\omega)$

Now, we consider the first diagonal element of $W_1(j\omega)$. Using the parameterizations given in (2), where

$$\Lambda_{1\omega} = \text{diag}\begin{pmatrix}\lambda_{1\omega,11}\\ \lambda_{1\omega,22}\\ \vdots\\ \lambda_{1\omega,nn}\end{pmatrix} \in \mathbf{\Lambda}_n \quad \text{and}$$

$$W_1(j\omega) = \text{diag}\begin{pmatrix}w_{1,11}(j\omega)\\ w_{1,22}(j\omega)\\ \vdots\\ w_{1,nn}(j\omega)\end{pmatrix} \in \mathscr{GH}_\infty{}^{n\times n},$$

we can write

$$\lambda_{1\omega,11} = |w_{1,11}(j\omega)|^{-2} \Leftrightarrow 10\log_{10}\lambda_{1\omega,11} = -20\log_{10}|w_{1,11}(j\omega)|.$$

Differentiating with respect to ν_ω, where $\nu_\omega = \log_{10}\omega$, we have

$$\begin{aligned}\frac{\mathrm{d}}{\mathrm{d}\nu_\omega}\left(20\log_{10}|w_{1,11}(j\omega)|\right) &= \frac{\mathrm{d}}{\mathrm{d}\nu_\omega}\left(-10\log_{10}\lambda_{1\omega,11}\right)\\ &= \left(\frac{-10}{\ln 10}\right)\frac{\mathrm{d}}{\mathrm{d}\nu_\omega}\left(\ln\lambda_{1\omega,11}\right)\\ &= \left(\frac{-10\lambda_{1\omega,11}^{-1}}{\ln 10}\right)\frac{\mathrm{d}\lambda_{1\omega,11}}{\mathrm{d}\nu_\omega}.\end{aligned} \tag{5}$$

The smoothness constraint for $|w_{1,11}(j\omega)|$ can be written as

$$\left|\frac{\mathrm{d}}{\mathrm{d}\nu_\omega}\left(20\log_{10}|w_{1,11}(j\omega)|\right)\right| < g_1(\omega),$$

where $g_1(\omega)$ (dB/decade) is the bound on the log–log gradient of the magnitude response of $w_{1,11}(j\omega)$. Without loss of generality, we have assumed the same bound on both positive and negative

gradients in the formulation via the imposition of the modulus sign.

Using the expression in (5), we have

$$\Leftrightarrow \left|\left(\frac{10\lambda_{1\omega,11}^{-1}}{\ln 10}\right)\frac{\mathrm{d}\lambda_{1\omega,11}}{\mathrm{d}\nu_\omega}\right| < g_1(\omega) \tag{6}$$

$$\Leftrightarrow \left|\frac{\mathrm{d}\lambda_{1\omega,11}}{\mathrm{d}\nu_\omega}\right| < \frac{\ln 10}{10}\lambda_{1\omega,11}g_1(\omega).$$

Now, considering the j-th and $(j-1)$-th point-wise in frequency grid points (denoted as ω_j and ω_{j-1}, respectively), which are very close to each other, and using differentiation from first principles, we have

$$\left|\lim_{\nu_{\omega_j}\to\nu_{\omega_{j-1}}}\frac{\lambda_{1\omega_j,11}-\lambda_{1\omega_{j-1},11}}{\nu_{\omega_j}-\nu_{\omega_{j-1}}}\right| < \frac{\ln 10}{10}\lambda_{1\omega_{j-1},11}g_1(\omega_j).$$

Denoting $\nu_{\omega_j}-\nu_{\omega_{j-1}}$ by $\delta\nu$ (assuming constant spaced gridding on a log scale) and squaring both sides, we have

$$\Leftrightarrow \left(\lambda_{1\omega_j,11}-\lambda_{1\omega_{j-1},11}\right)^2 - \left(\frac{\ln 10}{10}\lambda_{1\omega_{j-1},11}g_1(\omega_j)\delta\nu\right)^2 < 0$$

$$\Leftrightarrow \left(\frac{\ln 10}{10}\lambda_{1\omega_{j-1},11}g_1(\omega_j)\delta\nu\right) - \left(\lambda_{1\omega_j,11}-\lambda_{1\omega_{j-1},11}\right) \times \left(\frac{\ln 10}{10}\lambda_{1\omega_{j-1},11}g_1(\omega_j)\delta\nu\right)^{-1}\left(\lambda_{1\omega_j,11}-\lambda_{1\omega_{j-1},11}\right) > 0.$$

Consequently, the smoothness constraint for the other diagonal elements of $W_1(j\omega)$ can be written as follows:

$$\left(\frac{\ln 10}{10}\lambda_{1\omega_{j-1},22}g_1(\omega_j)\delta\nu\right) - \left(\lambda_{1\omega_j,22}-\lambda_{1\omega_{j-1},22}\right) \times \left(\frac{\ln 10}{10}\lambda_{1\omega_{j-1},22}g_1(\omega_j)\delta\nu\right)^{-1}\left(\lambda_{1\omega_j,22}-\lambda_{1\omega_{j-1},22}\right) > 0$$

$$\vdots$$

$$\left(\frac{\ln 10}{10}\lambda_{1\omega_{j-1},nn}g_1(\omega_j)\delta\nu\right) - \left(\lambda_{1\omega_j,nn}-\lambda_{1\omega_{j-1},nn}\right) \times \left(\frac{\ln 10}{10}\lambda_{1\omega_{j-1},nn}g_1(\omega_j)\delta\nu\right)^{-1}\left(\lambda_{1\omega_j,nn}-\lambda_{1\omega_{j-1},nn}\right) > 0.$$

The above inequalities can equivalently be represented in matrix form as Eq. (7), given in Box I for ease of representation.

Now, using the Schur complement lemma [14] on (7), the smoothness constraint for W_1 can be written in LMI form as follows:

$$\Leftrightarrow \begin{bmatrix} \frac{\ln 10}{10}\Lambda_{1\omega_{j-1}}g_1(\omega_j)\delta\nu & \left(\Lambda_{1\omega_j}-\Lambda_{1\omega_{j-1}}\right) \\ \left(\Lambda_{1\omega_j}-\Lambda_{1\omega_{j-1}}\right) & \frac{\ln 10}{10}\Lambda_{1\omega_{j-1}}g_1(\omega_j)\delta\nu \end{bmatrix} > 0. \tag{8}$$

The above constraint can be implemented on finite frequency grid points specified by the designer. Thus, the gradient of the magnitude response of $W_1(j\omega)$ is bounded by $g_1(\omega)$ at all frequency grid points.

3.2. Smoothness constraint for the diagonal post-compensator $W_2(j\omega)$

Similar to the formulation for the pre-compensator $W_1(j\omega)$, we first consider the first diagonal element of $W_2(j\omega)$, and based on (2), we can write

$$\lambda_{2\omega,11} = |w_{2,11}(j\omega)|^2 \Leftrightarrow 10\log_{10}\lambda_{2\omega,11} = 20\log_{10}|w_{2,11}(j\omega)|.$$

Differentiating with respect to ν_ω, we have

$$\begin{aligned}\frac{\mathrm{d}}{\mathrm{d}\nu_\omega}\left(20\log_{10}|w_{2,11}(j\omega)|\right) &= 10\frac{\mathrm{d}}{\mathrm{d}\nu_\omega}\left(\log_{10}\lambda_{2\omega,11}\right)\\ &= \left(\frac{10}{\ln 10}\right)\frac{\mathrm{d}}{\mathrm{d}\nu_\omega}\left(\ln\lambda_{2\omega,11}\right)\\ &= \left(\frac{10\lambda_{2\omega,11}^{-1}}{\ln 10}\right)\frac{\mathrm{d}\lambda_{2\omega,11}}{\mathrm{d}\nu_\omega}.\end{aligned} \tag{9}$$

The smoothness constraint for $|w_{2,11}(j\omega)|$ can similarly be written as

$$\left|\frac{\mathrm{d}}{\mathrm{d}\nu_\omega}\left(20\log_{10}|w_{2,11}(j\omega)|\right)\right| < g_2(\omega),$$

where $g_2(\omega)$ (dB/decade) is the bound on the log–log gradient of the magnitude response of $w_{2,11}(j\omega)$.

Using the expression in (9), we have

$$\Leftrightarrow \left|\frac{10\lambda_{2\omega,11}^{-1}}{\ln 10}\frac{\mathrm{d}\lambda_{2\omega,11}}{\mathrm{d}\nu_\omega}\right| < g_2(\omega).$$

This constraint is in the same form as that formulated for $W_1(j\omega)$ in (6). Therefore, the complete smoothness constraint for $W_2(j\omega)$ can similarly be written in an LMI framework as follows:

$$\begin{bmatrix} \frac{\ln 10}{10}\Lambda_{2\omega_{j-1}}g_2(\omega_j)\delta\nu & \left(\Lambda_{2\omega_j}-\Lambda_{2\omega_{j-1}}\right) \\ \left(\Lambda_{2\omega_j}-\Lambda_{2\omega_{j-1}}\right) & \frac{\ln 10}{10}\Lambda_{2\omega_{j-1}}g_2(\omega_j)\delta\nu \end{bmatrix} > 0. \tag{10}$$

For $W_1(j\omega)$ and $W_2(j\omega)$, the formulated LMI constraints (8) and (10), respectively, are imposed on frequency grid point ω_j with respect to ω_{j-1}. For a finite number of frequency grid points specified by the designer, these two constraints ensure smoothness in the magnitude plot of the compensators by restricting the gradient at each frequency grid point within a specified bound. Hence, the existing algorithm of Lanzon [5], in addition to these two constraints, results in a complete weight optimization framework for $\mathscr{H}_\infty$ loop-shaping control for the synthesis of smooth weights and a stabilizing controller.

4. Solution algorithm

A sub-optimal solution based on the formulation given in the last two sections is proposed for optimization problem (4). Since the posed problem is not simultaneously convex in all variables, an iterative algorithm must be used to solve the optimization problem. The inputs to the algorithm are (i) a scaled nominal plant $P \in \mathscr{R}^{m\times n}$, where[2] $m \geq n$, (ii) frequency functions $\underline{s}$ and $\overline{s}$, which are the boundaries for an allowable loop shape, (iii) frequency functions $\underline{w}_i$ and $\overline{w}_i$, which delimit the allowable region for the singular values of loop-shaping weight W_i $(i = 1, 2)$, (iv) frequency function k_i, which provides bound for the condition number of loop-shaping weight W_i $(i = 1, 2)$ and (v) frequency function g_i, which delimits the gradient of loop-shaping weight W_i $(i = 1, 2)$.

The solution algorithm is hereby presented as follows.

1. Find a controller $C_0^\star(j\omega)$ (as a feasible initial starting point for the algorithm) such that the interconnection $\left[P, C_0^\star\right]$ is internally stable. Set $i = 0$, where i denotes the iteration number, and let $\varepsilon_{\max,0}^\star = -1$.

[2] This ensures that the plant is square or tall. If it is fat, one can easily consider the dual problem where $W_1 = W_2^T$, $W_2 = W_1^T$, $P = P^T$ and $C_\infty = C_\infty^T$, and so there is no loss of generality in imposing this constraint.

$$\operatorname{diag}\begin{pmatrix}\left(\frac{\ln 10}{10}\lambda_{1\omega_{j-1},11}g_1(\omega_j)\delta\nu\right)-\left(\lambda_{1\omega_j,11}-\lambda_{1\omega_{j-1},11}\right)\left(\frac{\ln 10}{10}\lambda_{1\omega_{j-1},11}g_1(\omega_j)\delta\nu\right)^{-1}\left(\lambda_{1\omega_j,11}-\lambda_{1\omega_{j-1},11}\right)\\ \left(\frac{\ln 10}{10}\lambda_{1\omega_{j-1},22}g_1(\omega_j)\delta\nu\right)-\left(\lambda_{1\omega_j,22}-\lambda_{1\omega_{j-1},22}\right)\left(\frac{\ln 10}{10}\lambda_{1\omega_{j-1},22}g_1(\omega_j)\delta\nu\right)^{-1}\left(\lambda_{1\omega_j,22}-\lambda_{1\omega_{j-1},22}\right)\\ \vdots\\ \left(\frac{\ln 10}{10}\lambda_{1\omega_{j-1},nn}g_1(\omega_j)\delta\nu\right)-\left(\lambda_{1\omega_j,nn}-\lambda_{1\omega_{j-1},nn}\right)\left(\frac{\ln 10}{10}\lambda_{1\omega_{j-1},nn}g_1(\omega_j)\delta\nu\right)^{-1}\left(\lambda_{1\omega_j,nn}-\lambda_{1\omega_{j-1},nn}\right)\end{pmatrix}>0$$

$$\Leftrightarrow \frac{\ln 10 g_1(\omega_j)\delta\nu}{10}\operatorname{diag}\begin{pmatrix}\lambda_{1\omega_{j-1},11}\\ \lambda_{1\omega_{j-1},22}\\ \vdots\\ \lambda_{1\omega_{j-1},nn}\end{pmatrix}-\left[\operatorname{diag}\begin{pmatrix}\lambda_{1\omega_j,11}\\ \lambda_{1\omega_j,22}\\ \vdots\\ \lambda_{1\omega_j,nn}\end{pmatrix}-\operatorname{diag}\begin{pmatrix}\lambda_{1\omega_{j-1},11}\\ \lambda_{1\omega_{j-1},22}\\ \vdots\\ \lambda_{1\omega_{j-1},nn}\end{pmatrix}\right]$$

$$\times\left[\frac{\ln 10 g_1(\omega_j)\delta\nu}{10}\operatorname{diag}\begin{pmatrix}\lambda_{1\omega_{j-1},11}\\ \lambda_{1\omega_{j-1},22}\\ \vdots\\ \lambda_{1\omega_{j-1},nn}\end{pmatrix}\right]^{-1}\left[\operatorname{diag}\begin{pmatrix}\lambda_{1\omega_j,11}\\ \lambda_{1\omega_j,22}\\ \vdots\\ \lambda_{1\omega_j,nn}\end{pmatrix}-\operatorname{diag}\begin{pmatrix}\lambda_{1\omega_{j-1},11}\\ \lambda_{1\omega_{j-1},22}\\ \vdots\\ \lambda_{1\omega_{j-1},nn}\end{pmatrix}\right]>0$$

$$\Leftrightarrow\left(\frac{\ln 10}{10}\Lambda_{1\omega_{j-1}}g_1(\omega_j)\delta\nu\right)-\left(\Lambda_{1\omega_j}-\Lambda_{1\omega_{j-1}}\right)\left(\frac{\ln 10}{10}\Lambda_{1\omega_{j-1}}g_1(\omega_j)\delta\nu\right)^{-1}\left(\Lambda_{1\omega_j}-\Lambda_{1\omega_{j-1}}\right)>0, \tag{7}$$

where

$$\Lambda_{1\omega_j}=\operatorname{diag}\begin{pmatrix}\lambda_{1\omega_j,11}\\ \lambda_{1\omega_j,22}\\ \vdots\\ \lambda_{1\omega_j,nn}\end{pmatrix}\quad\text{and}\quad\Lambda_{1\omega_{j-1}}=\operatorname{diag}\begin{pmatrix}\lambda_{1\omega_{j-1},11}\\ \lambda_{1\omega_{j-1},22}\\ \vdots\\ \lambda_{1\omega_{j-1},nn}\end{pmatrix}$$

Box I.

2. Increment i by 1.
3. Formulate and solve the following quasi-convex optimization problem at each frequency grid point ω_j, where $j=1,2,\ldots,N$ and N is selected by the designer:

   Minimize $\gamma_{\omega_j}^2$

   such that $\exists\Lambda_{1\omega_j}\in\mathbf{\Lambda}_n,\ \Lambda_{2\omega_j}\in\mathbf{\Lambda}_m$ satisfying

   (a)
   $$\begin{bmatrix}0 & P(j\omega_j)\\ 0 & I\end{bmatrix}^*\begin{bmatrix}\Lambda_{2\omega_j} & 0\\ 0 & \Lambda_{1\omega_j}\end{bmatrix}\begin{bmatrix}0 & P(j\omega_j)\\ 0 & I\end{bmatrix}\le\gamma_{\omega_j}^2\begin{bmatrix}I & P(j\omega_j)\\ C_{i-1}^\star(j\omega_j) & I\end{bmatrix}^*\begin{bmatrix}\Lambda_{2\omega_j} & 0\\ 0 & \Lambda_{1\omega_j}\end{bmatrix}\times\begin{bmatrix}I & P(j\omega_j)\\ C_{i-1}^\star(j\omega_j) & I\end{bmatrix},$$

   (b) $\underline{s}(\omega_j)^2\Lambda_{1\omega_j}<P^*(j\omega_j)\Lambda_{2\omega_j}P(j\omega_j)<\bar{s}(\omega_j)^2\Lambda_{1\omega_j}$,

   (c) $\exists\underline{\xi}_{1\omega_j},\bar{\xi}_{1\omega_j}:\ \underline{\xi}_{1\omega_j}I<\Lambda_{1\omega_j}<\bar{\xi}_{1\omega_j}I,\ \overline{w}_1(\omega_j)^{-2}<\underline{\xi}_{1\omega_j},\ \bar{\xi}_{1\omega_j}<\underline{w}_1(\omega_j)^{-2},\ \bar{\xi}_{1\omega_j}<k_1(\omega_j)^2\underline{\xi}_{1\omega_j}$,

   (d) $\exists\underline{\xi}_{2\omega_j},\bar{\xi}_{2\omega_j}:\ \underline{\xi}_{2\omega_j}I<\Lambda_{2\omega_j}<\bar{\xi}_{2\omega_j}I,\ \underline{w}_2(\omega_j)^2<\underline{\xi}_{2\omega_j},\ \bar{\xi}_{2\omega_j}<\overline{w}_2(\omega_j)^2,\ \bar{\xi}_{2\omega_j}<k_2(\omega_j)^2\underline{\xi}_{2\omega_j}$,

   (e) $0<\begin{bmatrix}\frac{\ln 10}{10}\Lambda_{1\omega_{j-1}}g_1(\omega_j)\delta\nu & \left(\Lambda_{1\omega_j}-\Lambda_{1\omega_{j-1}}\right)\\ \left(\Lambda_{1\omega_j}-\Lambda_{1\omega_{j-1}}\right) & \frac{\ln 10}{10}\Lambda_{1\omega_{j-1}}g_1(\omega_j)\delta\nu\end{bmatrix}$ when $j>1$,

   (f) $0<\begin{bmatrix}\frac{\ln 10}{10}\Lambda_{2\omega_{j-1}}g_2(\omega_j)\delta\nu & \left(\Lambda_{2\omega_j}-\Lambda_{2\omega_{j-1}}\right)\\ \left(\Lambda_{2\omega_j}-\Lambda_{2\omega_{j-1}}\right) & \frac{\ln 10}{10}\Lambda_{2\omega_{j-1}}g_2(\omega_j)\delta\nu\end{bmatrix}$ when $j>1$.

   Denote by $\Lambda_{1\omega_j}^\star$ and $\Lambda_{2\omega_j}^\star$ the values of $\Lambda_{1\omega_j}$ and $\Lambda_{2\omega_j}$ ($j=1,2,\ldots,N$) that achieve the minimum $\gamma_{\omega_j}^2$ of the optimization problem.
4. Construct *diagonal* transfer function matrices $W_{1,i}^\star(s)$ and $W_{2,i}^\star(s)$ in $\mathscr{GH}_\infty$ by fitting stable minimum phase transfer functions to each magnitude function on the main diagonal of $(\Lambda_{1\omega_j}^\star)^{-1/2}$ and $(\Lambda_{2\omega_j}^\star)^{1/2}j=1,2,\ldots,N$, respectively.
5. Compute $b_{\text{opt}}(W_{2,i}^\star PW_{1,i}^\star)$ as detailed in [1], and let this value be denoted by $\varepsilon_{\max,i}^\star$. Furthermore, synthesize a controller $C_{\infty,i}^\star$ that achieves a robust stability margin $b(W_{2,i}^\star PW_{1,i}^\star, C_{\infty,i}^\star)=\varepsilon_{\max,i}^\star$, usually using the state-space formula given in [15, Theorem 6.3]. Set $C_i^\star=W_{1,i}^\star C_{\infty,i}^\star W_{2,i}^\star$.
6. Evaluate $(\varepsilon_{\max,i}^\star-\varepsilon_{\max,i-1}^\star)$. If this difference (which is always positive) is very small, for instance 0.01, and has remained this small for the last few iterations, then EXIT; otherwise return to Step 2.

The outputs from the algorithm are (i) the maximized value of $b_{\text{opt}}(P_s)$ obtained in the variable $\varepsilon_{\max,i}^\star$, (ii) smooth diagonal loop-shaping weights $W_{1,i}^\star$ and $W_{2,i}^\star$ that achieve $\varepsilon_{\max,i}^\star$ and (iii) controller $C_{\infty,i}^\star(s)$ that achieves $b(W_{2,i}^\star PW_{1,i}^\star, C_{\infty,i}^\star)=\varepsilon_{\max,i}^\star$. Being an ascent algorithm, the value of $\varepsilon_{\max,i}^\star$ is monotonically non-decreasing as i increases, and at each iteration, $\inf_{\omega_j}\left(\frac{1}{\gamma_{\omega_j}}\right)\ge\varepsilon_{\max,i-1}^\star$. However, note that the above iterative algorithm cannot guarantee convergence to the global maximum, and only monotonicity properties can be guaranteed. This algorithm is quite insensitive to the initial choice of stabilizing controller $C_0^\star$, which is probably due to the fact that the algorithm has enough freedom to rectify a poor choice of initial stabilizing controller at both optimization Steps 3 and 5 of each iteration.

Remark 1. (i) The quasi-convex problem of Step 3 of the algorithm can be solved using LMI routines. If the robust stability margin is maximized by solving the optimization problem at each frequency ω_j, i.e. as indicated in Step 3, the initial choice of $\Lambda_{1\omega_j}$ and $\Lambda_{2\omega_j}$ at frequency grid point $\omega_j = \omega_1$ restricts the solution within a cone and can possibly result in unnecessary infeasibility at frequencies corresponding to lightly damped poles/zeros of the plant. However, the LMIs at each frequency ω_j can all be packed together into a single LMI constraint and the optimization problem can be solved over all frequency grid points in one go, thereby avoiding the above difficulty. Note that circumventing this restriction as described above inevitably introduces a trade-off with the available memory and CPU time used to solve the optimization problem.

(ii) In the optimization problem, the number of decision variables is $N(m + n + 2q)$, where $q = 1$ when only one weight is synthesized and $q = 2$ when both weights are synthesized. This number thus increases with the dimension of the nominal plant and the number of grid points. The number of decision variables does not however depend on the order of the plant.

5. Numerical example

We consider a scaled SISO plant P which has lightly damped poles and zeros (with damping ratio of 0.02) at $s = -0.0283 \pm j1.4139$ and $s = -0.4 \pm j19.996$, respectively. The transfer function of the scaled nominal plant is given below, and the magnitude plot is shown in Fig. 3.

$$P = \frac{10\left(s^2 + 0.8s + 400\right)}{s^2\left(s^2 + 0.0566s + 2\right)}.$$

For this plant, loop-shaping weights and an $\mathscr{H}_\infty$ loop-shaping controller are to be synthesized such that the following desired closed-loop specifications are met: these specifications are captured via a requirement that the designed loop shape needs to live within the loop-shape boundaries $\underline{s}(\omega)$ and $\bar{s}(\omega)$ given as

$$\underline{s}(\omega) = \frac{\left|\frac{j\omega}{4} + 1\right|}{|j\omega|^2\left|\frac{j\omega}{10} + 1\right|^4} \quad \text{and} \quad \bar{s}(\omega) = \frac{80\left|\frac{j\omega}{2} + 1\right|^3}{|j\omega|^4\left|\frac{j\omega}{50} + 1\right|},$$

selected based on time-domain specifications, for instance, steady-state error, rise-time, percentage overshoot, and so on (see [2] for details of connection between time-domain and frequency-domain requirements). The post-compensator is fixed at $W_2 = 1$ for simplicity, and the solution algorithm formulated in the previous section is then used to simultaneously synthesize a pre-compensator W_1 and stabilizing controller C_∞. The frequency functions $\underline{w}_1, \overline{w}_1, k_1$ and g_1 that confine the singular values, condition number and the gradient of pre-compensator W_1 are chosen as 10^{-5}, 10^5, 5 and 80 dB/dec, respectively. Note that a different problem specification might require designers selecting more complicated (perhaps frequency-dependent) bounds.

Here, two cases are considered to illustrate the effectiveness of the smoothness constraint: $\mathscr{H}_\infty$ loop-shaping designs with and without the smoothness constraint. 200 equally spaced frequency grid points between $\omega = 10^{-1}$ and 10^2 rad/s on a logarithmic scale are used to formulate the quasi-convex optimization problem in Step 3, and the resulting LMIs are packed into a single optimization problem. A stabilizing controller with a poor robust stability margin $b(P, C)$ of 0.0772 is used to initialize the solution algorithm. For practical convergence of the solution algorithm, Case 1 (with smoothness constraint) and Case 2 (without smoothness constraint) require five and four iterations, respectively. The singular values of the synthesized pre-compensator W_1, the achieved loop shape and the singular values of the synthesized robust stabilizing controller C_∞ for both cases are shown in Fig. 4.

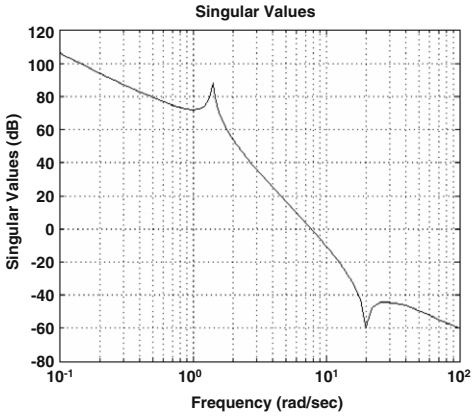

Fig. 3. Magnitude plot of the scaled nominal plant P.

It can be easily seen in the first case that the lightly damped poles and zeros of the nominal plant are retained in the shaped plant $P_s = W_2PW_1$ because the weights are smooth, while in the second case, the synthesized weight W_1 cancels these lightly damped poles and zeros. This results in a smooth $P_s = W_2PW_1$, which is undesirable, as there are lightly damped pole/zero cancellations when forming P_s which would make such a design fragile. In both simulations, the shaped plant lies in the specified region denoted by dashed lines in the second figure of each column of Fig. 4, and the roll-off rate around cross-over frequency is small. Also, the synthesized compensator W_1 in both cases has eight states with condition number less than 5 at all frequencies, which is considered good. The robust stability margins of 0.5907 and 0.7643 are obtained from Case 1 and Case 2, respectively, which are indicators of decent design. Indeed, more stringent performance specifications could have been demanded via tighter loop-shape boundary regions, as the robust stability margin is ample in both designs. Also, more importantly, notice that the gradient of the log-magnitude plot of the weight W_1 with respect to log-frequency is smaller at every frequency for Case 1 (with smoothness constraint incorporated) than for Case 2 (without smoothness constraint incorporated), as seen in the first figure of each column of Fig. 4. Indeed, Case 1 has no lightly damped peaks whereas Case 2 does. The solution algorithm when the optimization constraints are packed together (Case 1) takes approximately 15 min per iteration on a 2.66 GHz Intel® Core™ 2PC.

The transfer functions of the synthesized loop-shaping weights in Cases 1 and 2 are given in Box II.

6. Conclusion

Smoothness constraints have been formulated in LMI form and incorporated into a weight optimization framework for $\mathscr{H}_\infty$ loop-shaping control to synthesize smooth weights along with a stabilizing controller. The smoothness constraints limit the gradient with respect to log-frequency of the log-magnitude response of the synthesized weights, thereby preventing pole-zero cancellation of the nominal plant with the weights when the shaped plant is formed. The proposed algorithm therefore extends the applicability of this weight optimization framework to a larger class of LTI systems.

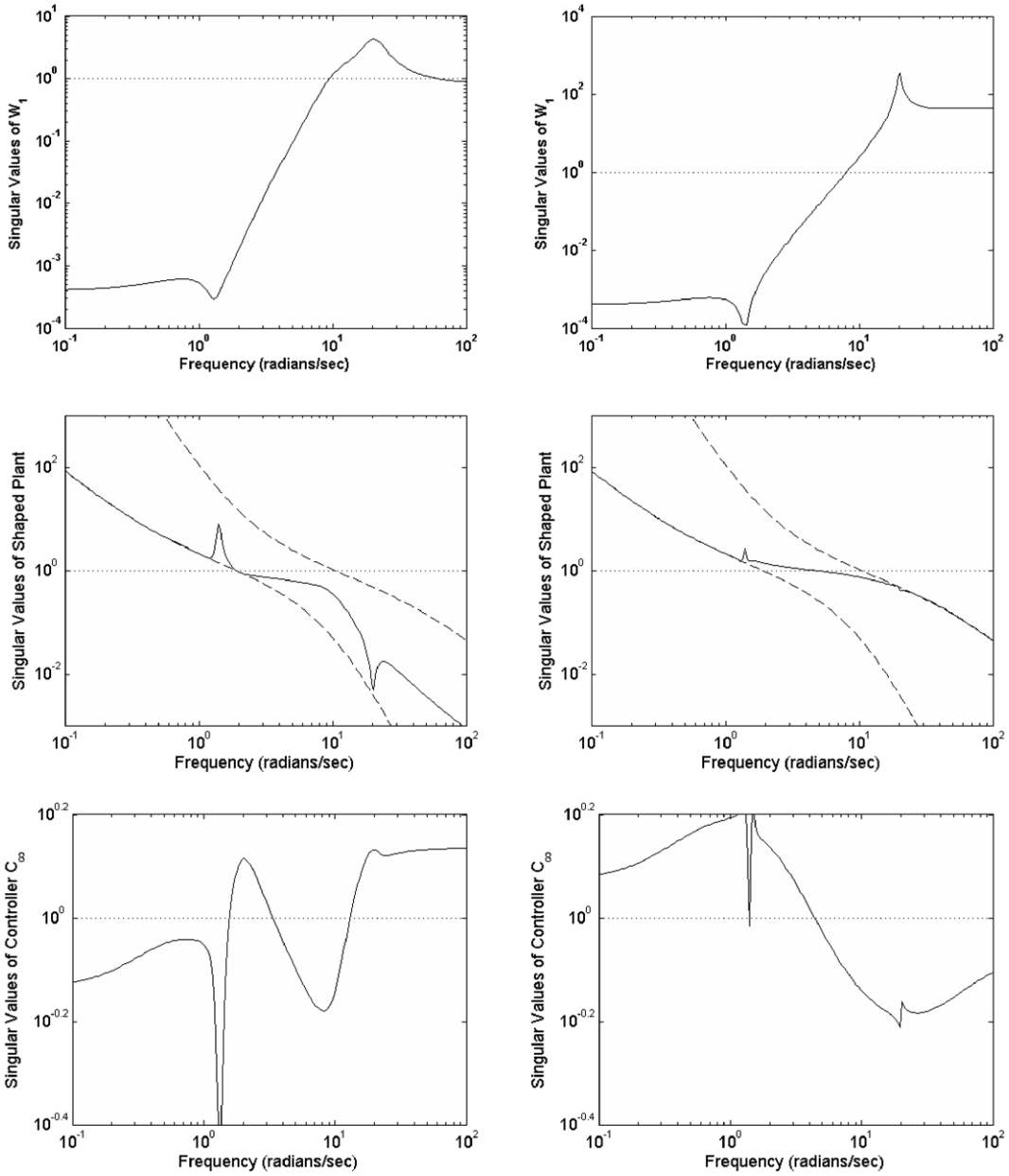

Fig. 4. Columns 1 and 2 correspond to Case 1 (with smoothness constraint) and Case 2, respectively.

$$\frac{0.8327s^8 + 34.42s^7 + 5171.1s^6 + 1718s^5 + 4022s^4 + 6549s^3 + 6591s^2 + 5735s + 1684}{s^8 + 30.67s^7 + 878.6s^6 + 13\,960s^5 + 142\,300s^4 + 957\,200s^3 + 3\,158\,000s^2 + 3\,829\,000s + 4124\,000e^6} \quad \text{and}$$

$$\frac{45.83s^8 + 1170s^7 + 3784s^6 + 8579s^5 + 15\,570s^4 + 19\,040s^3 + 17\,940s^2 + 13\,090s + 3305}{s^8 + 72.6s^7 + 2145s^6 + 41\,960s^5 + 696\,300s^4 + 4\,812\,000s^3 + 6\,200\,000s^2 + 9\,967\,000s + 8\,209\,000}$$

Box II.

Acknowledgements

The financial support of the Engineering and Physical Sciences Research Council and the Royal Society is gratefully acknowledged.

References

[1] K. Glover, D. McFarlane, Robust stabilization of normalized coprime factor plant descriptions with $\mathscr{H}_\infty$-bounded uncertainty, IEEE Transactions on Automatic Control 34 (8) (1989) 821–830.

[2] D. McFarlane, K. Glover, A loop-shaping design procedure using $\mathscr{H}_\infty$ synthesis, IEEE Transactions on Automatic Control 37 (6) (1992) 759–769.

[3] K. Zhou, J. Doyle, K. Glover, Robust and Optimal Control, Prentice Hall, Englewood Cliffs, NJ, 1996.

[4] G. Papageorgiou, K. Glover, A systematic procedure for designing non-diagonal weights to facilitate $\mathscr{H}_\infty$ loop shaping, in: Proceedings of IEEE CDC, San Diego, CA, US, 1997, pp. 2127–2132.

[5] A. Lanzon, Weight optimisation in $\mathscr{H}_\infty$ loop-shaping, Automatica 41 (1) (2005) 1201–1208.

[6] M. Tsai, E. Geddes, I. Postlethwaite, Pole-zero cancellations and closed-loop properties of an $\mathscr{H}_\infty$ mixed sensitivity design problem, in: Proceedings of IEEE CDC, Honolulu, HI, USA, 1990, pp. 1028–1029.

[7] P. Coustal, J. Michelin, Industrial application of an $\mathscr{H}_\infty$ design method for flexible structures, IEEE Control Systems Magazine 14 (4) (1994) 49–54.

[8] R. Middleton, S. Graebe, Slow stable open-loop poles: to cancel or not to cancel, Automatica 35 (5) (1999) 877–886.
[9] M. Turner, D. Bates, $\mathscr{H}_\infty$ control design, in: Mathematical Methods for Robust and Nonlinear Control, Springer, 2007.
[10] J. Sikaundi, M. Braae, Preventing pole-zero cancellation for improved input disturbance rejection in iterative feedback tuning systems, in: Novel Algorithms and Techniques in Telecommunications, Automation and Industrial Electronics, Springer, 2008.
[11] G. Vinnicombe, Uncertainty and Feedback: $\mathscr{H}_\infty$ Loop-Shaping and v-Gap Metric, Imperial College Press, 2001.
[12] R. Smith, C. Chu, J.L. Fanson, The design of $\mathscr{H}_\infty$ controllers for an experimental non-collocated flexible structure problem, IEEE Transactions on Control Systems Technology 2 (2) (1994).
[13] A. Preumont, Vibration Control of Active Structures, 2nd ed., Kluwer Academic Publishers, 2003.
[14] R. Horn, C. Johnson, Matrix Analysis, Cambridge University Press, 1996.
[15] K. Glover, All optimal Hankel-norm approximations of linear multivariable systems and their $\mathscr{L}_\infty$-error bounds, International Journal of Control 39 (6) (1984) 1115–1193.